Indian Geotech J (December 2021) 51(6):1319–1337
https://doi.org/10.1007/s40098-021-00534-7

ORIGINAL PAPER

Seismic Bearing Capacity of Shallow Foundations Placed on an Anisotropic and Nonhomogeneous Inclined Ground

Hamed Haghsheno[1] · **Mahyar Arabani**[1]

Received: 23 September 2020 / Accepted: 8 April 2021 / Published online: 21 April 2021

Abstract In the present study, the limit equilibrium method combined with the pseudo-static seismic loading approach and applying the simplified Coulomb failure mechanism were employed for calculating the bearing capacity of nonhomogeneous and anisotropic soils on slopes. It was assumed that the cohesion coefficient was nonhomogeneous and anisotropic and anisotropy effect was ignored for the friction angle. For estimating optimal bearing capacity values, the particle swarm optimization algorithm was used. Comparing the results of previous researchers with those of the present study for isotropic and homogeneous soils indicated that the present solution provided acceptable values for the bearing capacity of shallow foundations. The effect of anisotropy ratio and the nonhomogeneous coefficient on the seismic bearing capacity was evaluated and found that decreasing the anisotropy ratio and increasing the nonhomogeneous coefficient cause an increase in the seismic bearing capacity. Furthermore, the results showed that the depth of the failure zone decreases with increasing the nonhomogeneous coefficient, the anisotropy ratio, and the seismic acceleration coefficient, while the depth of the failure zone increases with an increase in the slope inclination.

Keywords Seismic bearing capacity · Shallow foundations · Slope · Nonhomogeneous and anisotropic soils · Limit equilibrium method

✉ Hamed Haghsheno
haghsheno@phd.guilan.ac.ir

Mahyar Arabani
arabani@guilan.ac.ir

[1] Department of Civil Engineering, Faculty of Engineering, University of Guilan, Rasht, Iran

List of Symbols

c_i	The cohesion corresponding to an inclination i
c_{v}	The cohesion coefficients in the vertical direction
c_{h}	The cohesion coefficients in the horizontal direction
K	The anisotropy coefficient
υ	The nonhomogeneous coefficient
i	The angle between the horizontal direction and the maximum principal stress
N_c	Bearing capacity factor
N_γ	Bearing capacity factor
γ	The unit weight of the soil
c_{h0}	The cohesion coefficient in the horizontal direction in $h = 0$
λ	The variation of the cohesion coefficient with depth
B_0	Width of the footing
P_{U}	The ultimate vertical load on the foundation
β	The slope inclination
q_{ult}	The ultimate bearing capacity of the strip footing
α_{A}	Slip surface angle in the active zone
α_{B}	Slip surface angle in the passive zone
φ	Angle of internal friction of soil
δ	The friction angle along the surface between the active and passive zones
P_{a}	The active thrust

P_p	The passive resistance
k_v	The vertical seismic acceleration coefficient
k_h	The horizontal seismic acceleration coefficient
h	The depth of failure zone
W_A	Weight of triangular wedge AEC
W_B	Weight of triangular wedge BEC
C_{AE}, C_{EB} and C_{CE}	The cohesion coefficient components

Introduction

The ultimate bearing capacity of a shallow foundation is a very important concept that every civil engineer faces when designing the structures. Many investigators have studied the static and seismic bearing capacity of shallow foundation rested on the horizontal ground [1–10]. Because some structures are built near the slope or on the slope, many authors [11–13] evaluated the behavior of shallow foundations near or on slopes under static conditions. Some researchers have analyzed the seismic bearing capacity of shallow strip footings near the slope or on the slope using the pseudo-static approach combined with different solution techniques such as limit equilibrium method [14–22], the method of stress characteristics [23–26], the lower bound [27–32], and the upper bound [33–39]. The studies indicated that the seismic bearing capacity of a shallow foundation located near the slope was significantly affected by the slope angle, the seismic acceleration coefficient, the distance between the shallow foundation edge, and the edge of the slope. Also, they have shown that the bearing capacity of a footing decreases with an increase in the horizontal seismic acceleration coefficient. Natural soil deposits are anisotropic and nonhomogeneous with respect to the cohesion coefficient [40–43]. Anisotropy as a basic property of materials considerably affects the bearing capacity of foundations [44]. Due to soil anisotropy, the undrained shear strength changes with failure plane orientation. In the problem of bearing capacity, along with any assumed failure surface, the direction of the principal stresses varies from one point to another. Hence, using the strength values of each orientation of the failure surface would result in more realistic results. Calculation of bearing capacity in this manner is of great importance, particularly for analytical solutions in which the undrained bearing capacity highly depends on one soil parameter (i.e., undrained shear strength) [45].

A few studies have evaluated the effect of nonhomogeneity and anisotropy on the bearing capacity of foundation on the horizontal ground rested on clay [46–61] and (c-φ) soil [62, 63].

Skempton [60] calculated the bearing capacity of a foundation on nonhomogeneous clays using empirical formulas. By considering the circular mechanism failure, Raymond [52] provided a solution for estimating the bearing capacity of surface footing on a frictionless soil, assuming a linear cohesion coefficient variation with depth. Bearing capacity of shallow strip footings on nonhomogeneous and anisotropic clays was analyzed by Sreenivasulu and Ranganatham [61] on the assumption of the cylindrical failure surface. By using the limit equilibrium approach and considering a circular failure surface, Menzies [51] presented a correction factor for the effect of cohesion coefficient anisotropy on the bearing capacity of a foundation. Reddy and Srinivasan [55, 56] analyzed the bearing capacity of footings over a single layer and also a two-layered nonhomogeneous and anisotropic clay by assuming a circular failure mechanism. By using circular failure mechanism, Reddy and Srinivasan [54] evaluated the effect of nonhomogeneity and anisotropy on the bearing capacity of c-φ soils, including $\varphi = 0$ conditions of soils. By considering a circular failure mechanism and using the upper bound analysis, Chen [59] analyzed the bearing capacity of footing on a single layer and a two-layered nonhomogeneous and anisotropic clay. Although the mathematical analysis is simplified by using the circular mechanism, the best solution is not provided by this mode of failure. Using the slip-line method, a correction coefficient for the bearing capacity foundation on anisotropic clays as a function of the soil strength parameters was proposed by Davis and Christian [48]. Appling the method of characteristic line, Davis and Booker [47] studied the effect of nonhomogeneous clays on the bearing capacity of foundation. Salencon [57] analyzed the bearing capacity of clay taking the variation of cohesion with depth as linear by using upper bound limit analysis. Using limit analysis and assuming a mechanism similar to Prandtl-type mechanism, Reddy and Rao [53] analyzed the bearing capacity of strip footing resting on nonhomogeneous and anisotropic clays. Gourvenec and Randolph [49] analyzed the bearing capacity of strip foundations and circular foundations on nonhomogeneous clays by applying the finite element method. By applying the upper bound approach of limit analysis and considering a translational failure mechanism, Al-Shamrani [46] presented closed-form solutions for the undrained bearing capacity of shallow strip footings on anisotropic clays. Al-Shamrani and Moghal [45] presented a closed-form solution based on the kinematical approach of limit analysis for the undrained bearing capacity of strip footings on anisotropic cohesive soils. Using the discrete element method (DEM) in the framework of the upper bound theory of limit analysis, Yang and Du [58] investigated the effect of nonhomogeneous and anisotropic soils on the bearing capacity coefficient of strip foundation. By applying the limit equilibrium method associated with the Coulomb failure mechanism, Izadi et al. [50] evaluated the effect of variation of cohesion coefficient of marine deposit with a depth on seismic bearing capacity. Meyerhof [62] obtained the bearing capacity of soils with anisotropy in friction by the conventional Terzaghi's type approach. For this purpose, two extreme values of φ for the outer zones and equivalent φ for the radial shear zone was considered. Applying the upper bound approach of limit analysis and a mechanism similar to Prandtl-type mechanism, Reddy and Rao [63] evaluated the bearing capacity of nonhomogeneous and anisotropic (c-φ) soils. All mentioned investigations indicate that nonhomogeneity and anisotropy have a notable effect on the bearing capacity of the soils.

However, not much research has been done on the effect of nonhomogeneous and anisotropic soil on the bearing capacity of a foundations near or on slopes. Halder and Chakraborty [64], using the lower bound limit analysis technique, evaluated the bearing capacity of a strip footing placed over an embankment of anisotropic clay. It was shown that the anisotropy ratio has a significant effect on the bearing capacity of the shallow foundation. The main objective of the present research is to evaluate the effect of anisotropic and nonhomogeneous soil on the bearing capacity of a strip foundation on a slope. For this purpose, the simplified Coulomb failure mechanism and the limit equilibrium method of analysis, which have not been used in any of the previous studies for this purpose, were utilized. The cohesion coefficient was assumed to be nonhomogeneous and anisotropic. A two-wedge failure mechanism, proposed by Richards et al. [6], was adopted. It should be noted that this failure mechanism was applied by Ghazavi and Eghbali [65] and Ghosh and Debnath [3] to evaluate the bearing capacity of a shallow foundation rested on the horizontal ground. Comparing the results obtained by these researchers with the Finite Element analyses revealed that using this failure mechanism provided acceptable results. The PSO algorithm and MATLAB MathWorks were applied for the optimization in the present solution. Comprehensive comparisons were made with the results of previous studies. Furthermore, the effect of the nonhomogeneity and the anisotropy on bearing capacity factors and the depth and path of the failure zone was evaluated.

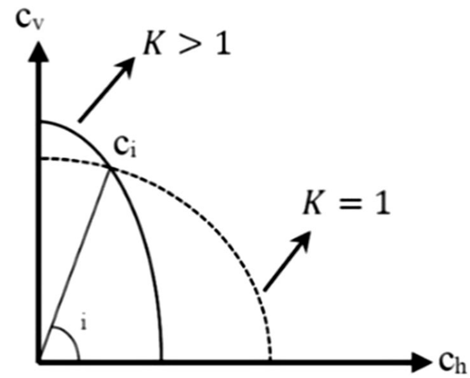

Fig. 1 Anisotropy of the cohesion coefficient

Anisotropy and Nonhomogeneity of Soil

Figure 1 presents the changing pattern of cohesion coefficient anisotropy, based on Casagrande [41], Livneh and Komornik [42], Reddy and Rao [53, 63], and Livneh and Greenstein [66]. The variation of cohesion coefficient with the angle of inclination (i) is given by:

$$c_i = c_{\mathrm{h}} + (c_{\mathrm{h}} - c_{\mathrm{v}})\sin^2 i = c_{\mathrm{h}}\left(1 + (K - 1)\sin^2 i\right) \tag{1}$$

where c_i is the cohesion corresponding to an inclination i, c_{h} and c_{v} are the cohesion coefficients in the horizontal and vertical directions, respectively, i is the angle between the horizontal direction and the maximum principal stress and K is the anisotropy coefficient, which is $c_{\mathrm{v}}/c_{\mathrm{h}}$.

The changing pattern of the nonhomogeneity of the cohesion coefficient is shown in Fig. 2.

From Fig. 2, it is clear that the variation of the cohesion coefficient with depth is assumed as linear. The cohesion coefficient at depth h from the surface is given by:

$$c_{\mathrm{h}} = c_{\mathrm{h}0} + \lambda h \tag{2}$$

where $c_{\mathrm{h}0}$ is the cohesion coefficient in the horizontal direction at $h = 0$ and λ is a variation of the cohesion coefficient with depth, which is suggested to be in the

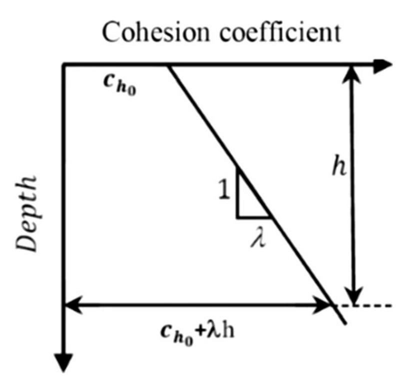

Fig. 2 Variation of cohesion coefficient with depth

range of 0.6–3 kPa/m by Tant and Craig [67] and 5 kPa/m by Wood [68].

Model Definition and Analysis of Procedure

In this study, a footing with the width of B_0 was placed horizontally on an inclined ground surface (Fig. 3). The bearing capacity of the strip footing (q_{ult}) is normally computed using the following basic formulation:

$$q_{\mathrm{ult}} = c_{\mathrm{v}} N_c + \frac{1}{2} B_0 \gamma N_\gamma \tag{3}$$

where N_c and N_γ are bearing capacity factors and γ is the unit weight of the soil.

The failure mechanism presented in Fig. 3 is almost similar to the original two-wedge slip surfaces proposed by Richards et al. [6]. Here, P_{U} is the vertical load on the foundation and β is the slope inclination. As shown in Fig. 3, the vertical surface CE is assumed to behave like a vertical retaining wall. At the failure stage, the weight of the wedge ACE and active pressure resulting from q_{ult} are applied from the left side on the wall. On the right-hand side, the weight of the wedge CBE applies lateral passive pressure on the virtual wall. To satisfy equilibrium, the active and passive thrusts acting on the virtual wall must be equal.

In the analytical solution, it is assumed that the failure mechanism consists of an active and passive wedge with their inclination angles considered as the variable of the present analysis. To determine the coefficients of bearing capacity, the failure-wedge geometry of the problem is depicted in Fig. 4. In this figure, φ is the friction angles of the soil; α_{A} is the slip surface angle in the active zone; α_{B} is slip surface angle in the passive zone; δ is the friction angle along the surface between the active and passive zones; k_{v} is the vertical seismic acceleration coefficient; k_{h} is the horizontal seismic acceleration coefficient; and h is the depth of failure zone.

P_{a} is the active thrust that acts on the active zone and P_{p} is the passive resistance exerted on the passive zone.

Using the limit equilibrium method and equating forces on the active and passive zones, the bearing capacity factor is obtained. In the active zone (Fig. 4a), by writing the forces in horizontal and vertical directions, P_{a} is obtained from Eqs. (4)-(9).

$$\begin{aligned}\sum H &= 0\\ &\Rightarrow R_{\mathrm{A}}\sin(\alpha_{\mathrm{A}}-\varphi) - C_{\mathrm{AE}}\cos\alpha_{\mathrm{A}} - P_{\mathrm{a}}\cos\delta\\ &\quad + (P_{\mathrm{u}}+W_{\mathrm{A}})k_{\mathrm{h}}\\ &= 0\end{aligned} \tag{4}$$

$$\begin{aligned}\sum V &= 0\\ &\Rightarrow R_{\mathrm{A}}\cos(\alpha_{\mathrm{A}}-\varphi) + C_{\mathrm{AE}}\sin\alpha_{\mathrm{A}} + C_{\mathrm{CE}}\\ &\quad - (P_{\mathrm{u}}+W_{\mathrm{A}})(1\pm k_{\mathrm{v}}) + P_{\mathrm{a}}\sin\delta\\ &= 0\end{aligned} \tag{5}$$

$$C_{\mathrm{AE}} = \frac{c_{\mathrm{h}}\left(1+(K-1)\sin^2\alpha_{\mathrm{A}}\right)h + 0.5\lambda h^2}{\sin\alpha_{\mathrm{A}}} \tag{6}$$

$$C_{\mathrm{CE}} = c_{\mathrm{h}} h K + 0.5h^2 = c_{\mathrm{v}} h + 0.5\lambda h^2 \tag{7}$$

$$W_{\mathrm{A}} = \frac{1}{2} B_0^2 \gamma \tan\alpha_{\mathrm{A}} \tag{8}$$

$$\begin{aligned}P_{\mathrm{a}} &= (P_{\mathrm{u}}+W_{\mathrm{A}})\left(\frac{(1\pm k_{\mathrm{v}})\sin(\alpha_{\mathrm{A}}-\varphi) + k_{\mathrm{h}}\cos(\alpha_{\mathrm{A}}-\varphi)}{\cos(\alpha_{\mathrm{A}}-\varphi-\delta)}\right)\\ &\quad - c_{\mathrm{h}}\left(1+(K-1)\sin^2\alpha_{\mathrm{A}}\right)h\left(\frac{\sin(\alpha_{\mathrm{A}}-\varphi)+\cot\alpha_{\mathrm{A}}\cos(\alpha_{\mathrm{A}}-\varphi)}{\cos(\alpha_{\mathrm{A}}-\varphi-\delta)}\right)\\ &\quad - \lambda h^2\left(\frac{\sin(\alpha_{\mathrm{A}}-\varphi)+0.5\cot\alpha_{\mathrm{A}}\cos(\alpha_{\mathrm{A}}-\varphi)}{\cos(\alpha_{\mathrm{A}}-\varphi-\delta)}\right) - Kc_{\mathrm{h}}h\frac{\sin(\alpha_{\mathrm{A}}-\varphi)}{\cos(\alpha_{\mathrm{A}}-\varphi-\delta)}\end{aligned} \tag{9}$$

where $h = B_0\tan\alpha_{\mathrm{A}}$ is the depth of the failure mechanism.

The same procedure is followed for the passive zone (Fig. 4b) and P_{p} is obtained from Eqs. (10)-(15).

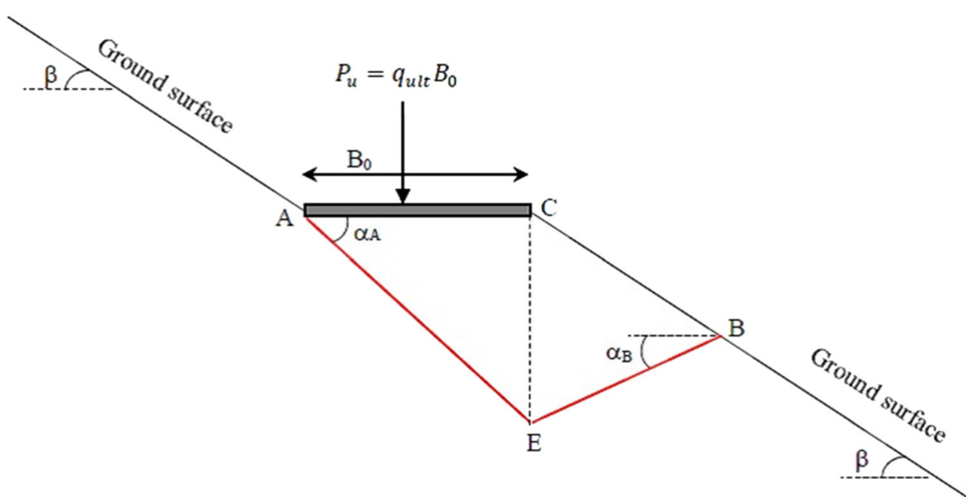

Fig. 3 Failure mechanism and wedges assumed in the present analysis

Fig. 4 Free body diagrams of the active and passive wedges

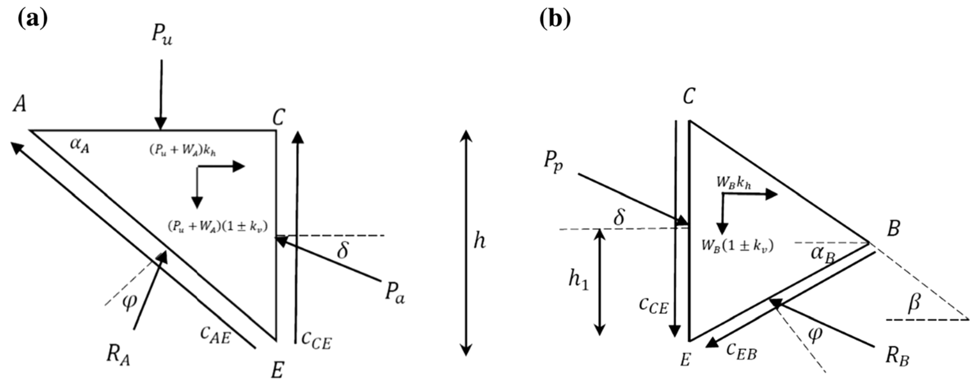

$$\sum H = 0 \Rightarrow P_p \cos\delta - R_B \sin(\alpha_B + \varphi) - C_{EB}\cos\alpha_B + W_B k_h = 0 \tag{10}$$

$$\sum V = 0 \Rightarrow R_B \cos(\alpha_B + \varphi) - W_B(1 \pm k_v) - P_p \sin\delta - C_{EB}\sin\alpha_B - C_{CE} = 0 \tag{11}$$

$$C_{EB} = \frac{c_h\left(1 + (K-1)\sin^2\alpha_B\right)h_1 + 0.5\lambda h_1^2}{\sin\alpha_B} \tag{12}$$

$$h_1 = \frac{B_0 \tan\alpha_A \tan\alpha_B}{\tan\alpha_B + \tan\beta} \tag{13}$$

$$W_B = \frac{1}{2}\frac{\gamma B_0^2 \tan^2\alpha_A}{\tan\alpha_B + \tan\beta} \tag{14}$$

$$\begin{aligned} P_p = {} & (W_B)\left(\frac{(1-k_v)\sin(\alpha_B+\varphi) - k_h\cos(\alpha_B+\varphi)}{\cos(\alpha_B+\varphi+\delta)}\right) + \frac{1}{2}\lambda h^2 \frac{\sin(\alpha_B+\varphi)}{\cos(\alpha_B+\varphi+\delta)} \\ & + c_h\left(1+(K-1)\sin^2\alpha_B\right)\left(\frac{B_0\tan\alpha_A\tan\alpha_B}{\tan\alpha_B+\tan\beta}\right)\left(\frac{\sin(\alpha_B+\varphi)+\cot\alpha_B\cos(\alpha_B+\varphi)}{\cos(\alpha_B+\varphi+\delta)}\right) \\ & + \frac{1}{2}\lambda\left(\frac{B_0\tan\alpha_A\tan\alpha_B}{\tan\alpha_B+\tan\beta}\right)^2\left(\frac{\sin(\alpha_B+\varphi)+\cot\alpha_B\cos(\alpha_B+\varphi)}{\cos(\alpha_B+\varphi+\delta)}\right) \\ & + Kc_h h\frac{\sin(\alpha_B+\varphi)}{\cos(\alpha_B+\varphi+\delta)} \end{aligned} \tag{15}$$

Given the equilibrium of two wedges, the active pressure and the passive resistance are equated. Therefore, by equating the active pressure and passive resistance, the ultimate bearing capacity (q_{ult}) can be obtained as follows:

$$P_a = P_p \tag{16}$$

$$q_{ult} = c_v N_c + \frac{1}{2}B0\gamma N_\gamma \tag{17}$$

$$N_c = v\left(\frac{f}{a}\right) + \frac{e}{a} \tag{18}$$

$$N_\gamma = \frac{b}{a} \tag{19}$$

where $\upsilon = \left(\frac{\lambda B_0}{c_h}\right)$ is the nonhomogeneous coefficient.

Detailed equations **for** a, b, d, e, and f are given in the "Appendix" section.

From Eqs. (18) and (19), it can be stated that the bearing capacity factors depend on c, φ, c_v, c_h, k_v, k_h, B_0, υ, K, α_A, α_B, λ, and β. Here, all the parameters are constant except α_A and α_B. Therefore, to find the optimum values of N_c and N_γ, the optimization process is performed in terms of α_A and α_B.

The particle swarm optimization (PSO) algorithm and MATLAB MathWorks were applied for the optimization. The PSO, initially developed by Kennedy and Eberhart [69], is a stochastic optimization technique that has been inspired by the behavior of bird flocking, fish schooling and swarming theory. In PSO, a group of specks flies in the job lookup distance to detect their optimum berth. Typically, this optimum berth is characterized by the optimum fitness function. In the PSO, some candidate particles or the potential solutions fly in the problem search space to ensure that their positions are optimum. This optimum position is usually characterized by the optimum of a fitness function. Let V and X denote a particle's velocity and position in a search space, respectively. Then, the velocity of the ith particle is delimited by $V_i = (v_{i1}; v_{i2}; v_{i3};...; v_{id})$ and the ith particle may be interpreted as $X_i = (x_{i1}; x_{i2}; x_{i3};...; x_{id})$. Also, d denotes the dimension of the problem. The best previous particle of the ith particle is recorded and expressed as $P_i = (p_{i1}; p_{i2}; p_{i3};...; p_{id})$. Here, the index of the best particle among the studied population is represented by $P_g = (p_{g1}, p_{g2}, p_{g3}...p_{gd})$. The position and velocity of each particle can be estimated using Eqs. (20) and (21):

$$X_{id} = X_{id} + V_{id} \tag{20}$$

$$V_{id} = \omega \times V_{id} + c_1 \times \text{rand} \times (P_{id} - X_{id}) + c_1 \times \text{rand} \times \left(P_{gd} - X_{id}\right) \tag{21}$$

In these equations, c_1 and c_2 are position constants known as acceleration coefficient, rand is a random number within the range [0,1], and ω is the inertia weight

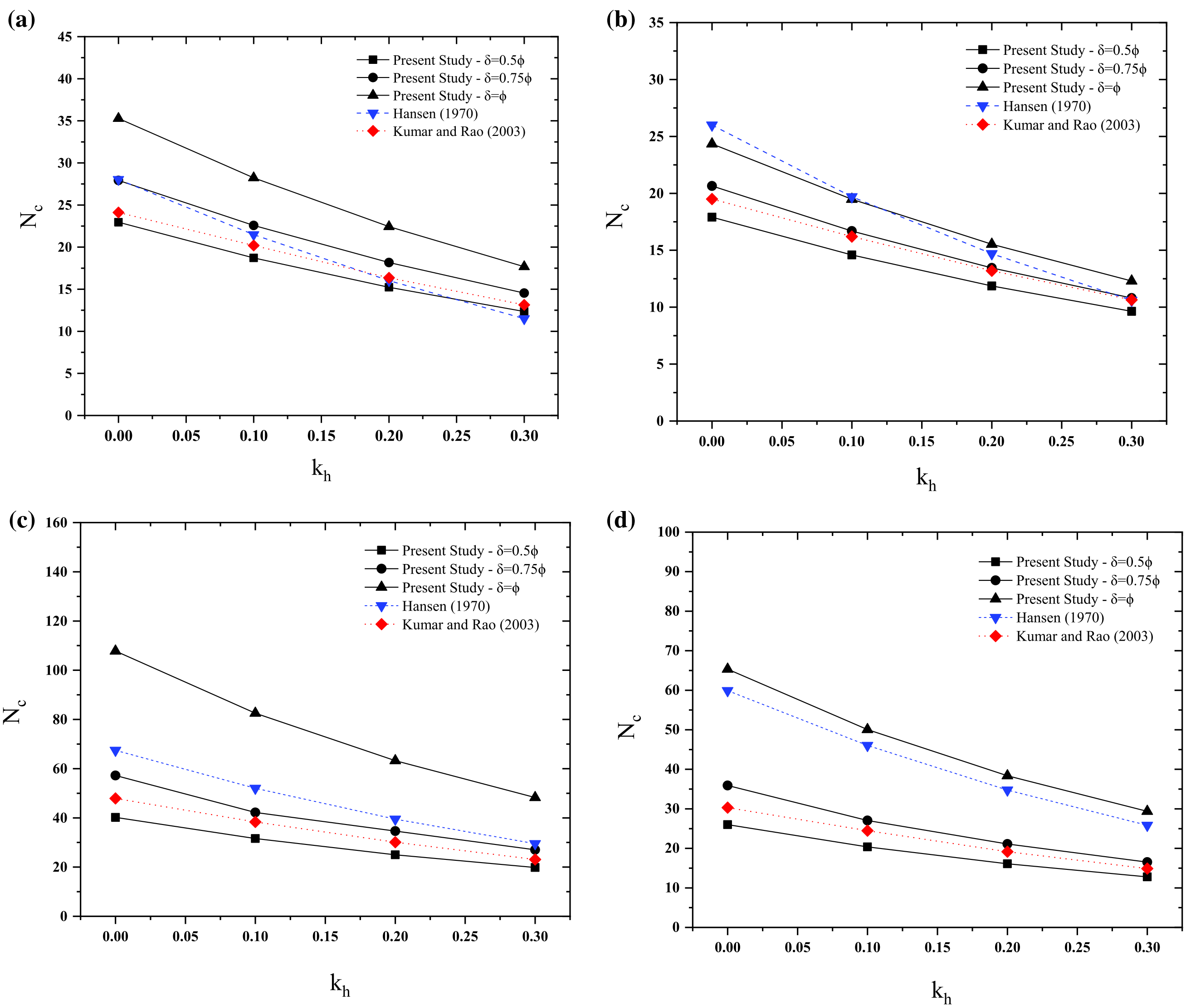

Fig. 5 Comparison of N_c with k_h and β for **a** φ = 30°, β = 10; **b** φ = 30°, β = 20; **c** φ = 40°, β = 15; **d** φ = 40°, β = 30

coefficient, which is calculated using the following equation:

$$\omega(\mathrm{gn}) = \omega_{\max} - \left[\frac{(\omega_{\max} - \omega_{\min})}{\mathrm{NI}}\right] * \mathrm{gn} \quad (22)$$

where gn is the generation.

The PSO is an appropriate algorithm to solve the low-dimensional problems like the topic of the present study. The efficiency of this algorithm to calculate the bearing capacity of the foundation was proved by Ghosh and Debnath [3] and Debnath and Ghosh [70, 71].

Comparisons

The results of estimated bearing capacity in the presence of k_h and β were compared with those of Hansen [12], Vesic [72], Zhu [10], Kumar and Rao [23], Kumar and Kumar [19] and Yamamoto [39] for the shallow foundation rested on anisotropic and nonhomogeneous soil. The comparison of the results is presented in Figs. 5 and 6. As can be inferred from Figs. 5 and 6, using different approaches for estimating the bearing capacity of shallow foundation rested near or on slopes gave a wide range of values for the bearing capacity factors. In some cases, the difference between the reported values is even more than 100%. This difference, in addition to the different approaches of determining the bearing capacity, is also related to using different failure mechanisms.

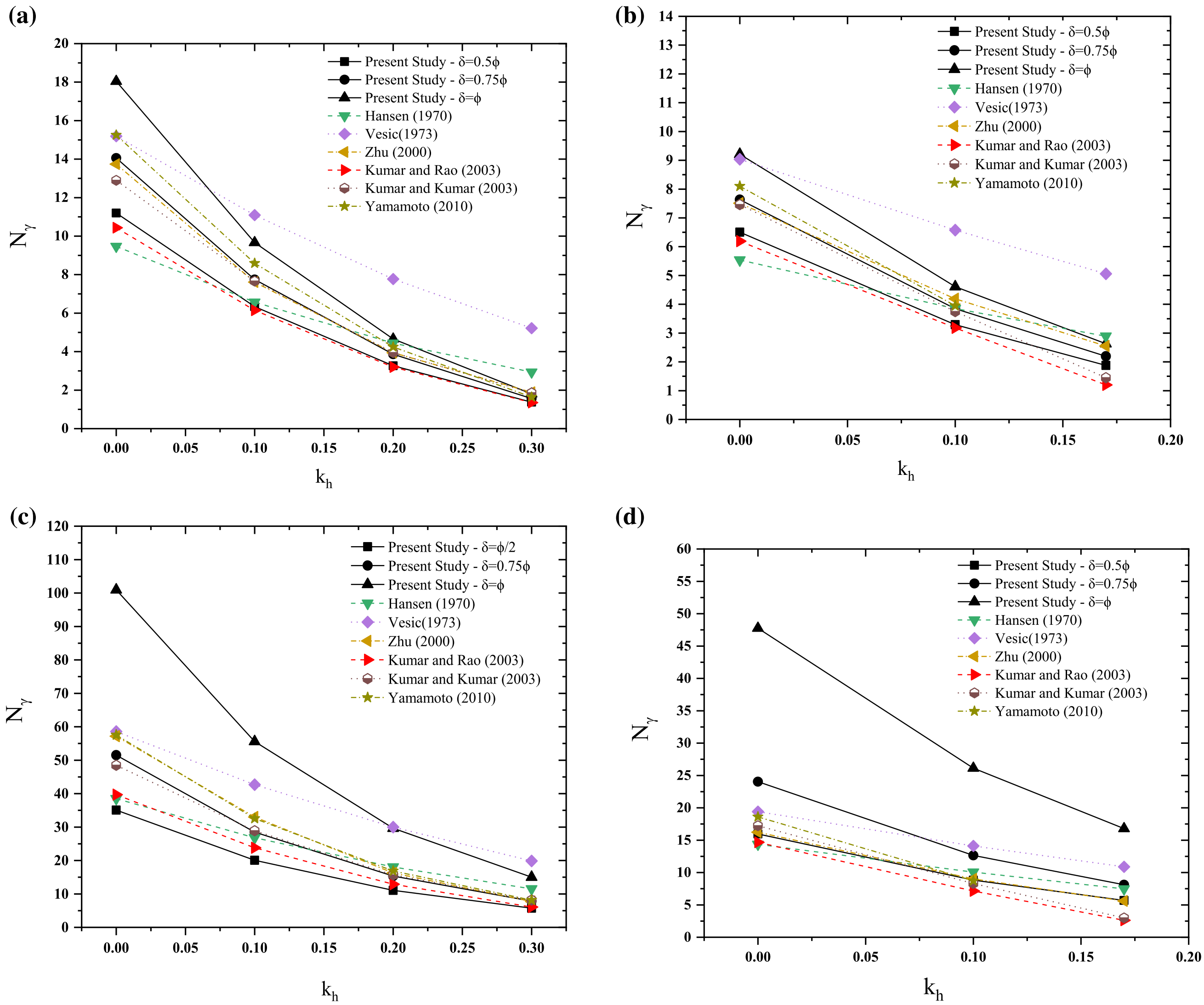

Fig. 6 Comparison of N_γ with k_h and β for **a** $\varphi = 30°$, $\beta = 10$; **b** $\varphi = 30°$, $\beta = 20$; **c** $\varphi = 40°$, $\beta = 15$; **d** $\varphi = 40°$, $\beta = 30$

Delta (δ) is a very effective parameter in the present analysis. Therefore, the results were assessed for three cases, namely $\delta = 0.5\varphi$, $\delta = 0.75\varphi$, and $\delta = \varphi$.

Figure 5 shows that the values of N_c provided by Kumar and Rao [23], who applied the method of stress characteristics, vary within the range of the present results from the cases $\delta = 0.5\varphi$ and $\delta = 0.75\varphi$. As reported by Kumar and Kumar [19] and Kumar and Ghosh [35], who, respectively, used the limit equilibrium method and the upper bound theory, the values of N_c obtained by them were close to those of Kumar and Rao [23]. Furthermore, Hansen [12] solution overestimated that of Kumar and Rao [23]. Overall, it can be concluded that when $\delta = 0.5\varphi$, the present solution is conservative. Moreover, when $\varphi = 40°$ and $\delta = \varphi$, the present solution overestimates those of Hansen [12] and Kumar and Rao [23]. One explanation for the difference between the results of the present study and those of the previous works may be using different failure mechanisms and methods. Figure 6 shows that when $\varphi = 30°$, the values of N_γ obtained by the present solution are close to those of Kumar and Rao [23] for the case $\delta = 0.5\varphi$; however, when $\delta = 0.75\varphi$, the values of N_γ of the present study are in good agreement with those of Zhu [10]. It should be noted that Zhu [10] employed the equivalence of limit equilibrium method and limit analysis to determine the bearing capacity factor, N_γ. Furthermore, Hansen [12] and Kumar and Rao [23] have minimum values under static and seismic conditions, respectively. When $\varphi = 40°$ and $\beta = 10°$, the values of N_γ obtained by Kumar and Rao [23] are within the range of the present results from the cases $\delta = 0.5\varphi$ and $\delta = 0.75\varphi$ while the results Zhu [10]and Yamamoto [39] are slightly higher than the present result for $\delta = 0.75\varphi$. It is of note that the solutions reported by Yamamoto [39] are based on the

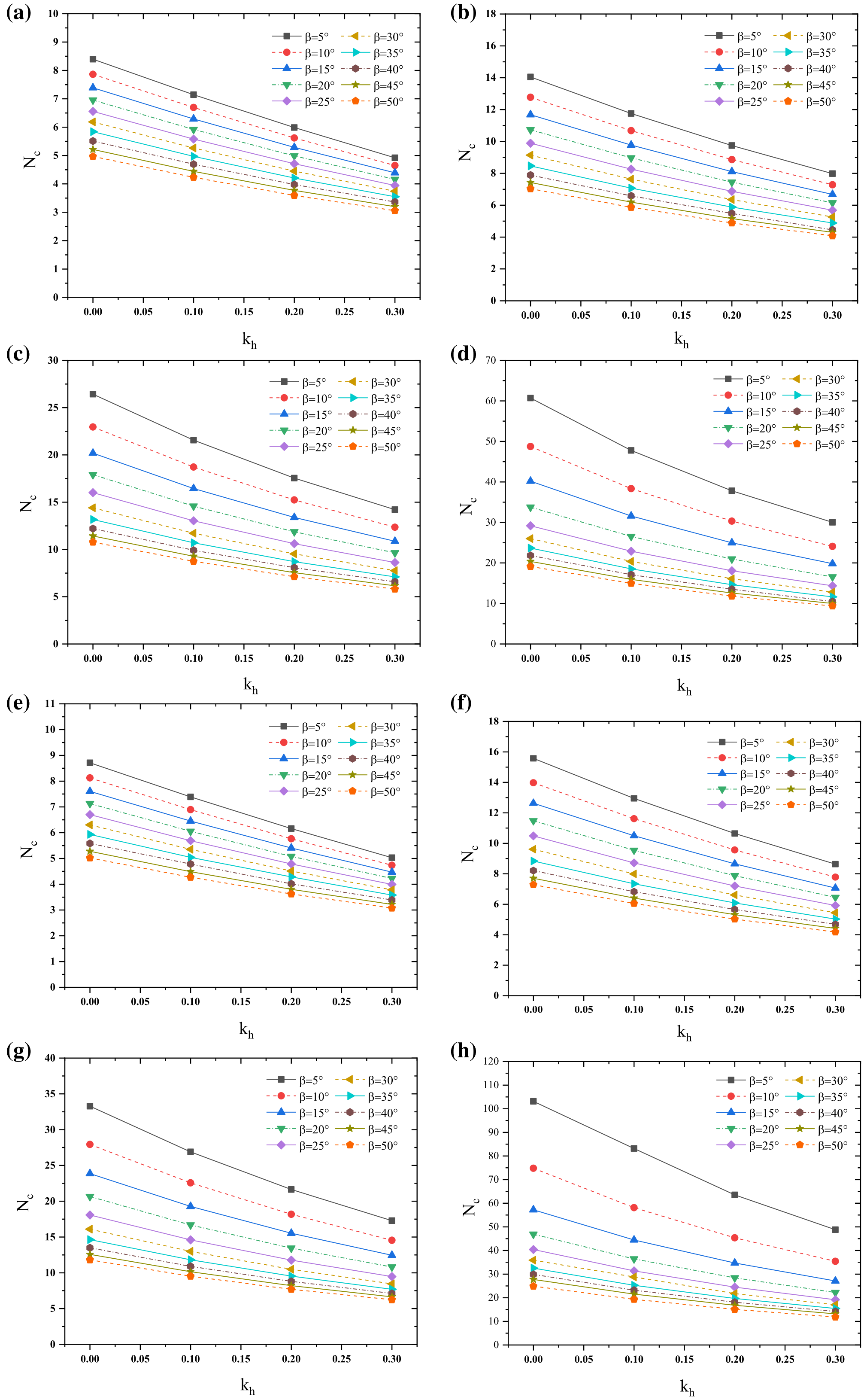

Fig. 7 Comparison of N_c with k_h and β for **a** φ = 10°, δ = 0.5φ; **b** φ = 20°, δ = 0.5φ; **c** φ = 30°, δ = 0.5φ; **d** φ = 40°, δ = 0.5φ; **e** φ = 10°, δ = 0.75φ; and **f** φ = 20°, δ = 0.75φ; g φ = 30°, δ = 0.75φ; h φ = 40°, δ = 0.75φ

upper bound method. By increasing the slope inclination to 20°, the results obtained by Hansen [12], Zhu [10], Kumar and Rao [23], Kumar and Kumar [19], and Yamamoto [39] are close to the present results for $\delta = 0.5\varphi$. According to Figs. 5 and 6 and considering that the obtained results depend on the amount of δ, it seems that acceptable values of the N_γ and N_c can be obtained between the results reported for $\delta = 0.5\varphi$ and $\delta = 0.75\varphi$.

As the merit of this study, the geometry of the failure mechanism is defined by only few angular parameters and the reason is employing the simple failure mechanism. Moreover, since other techniques need several other assumptions, the features of those solutions might be changeable.

Results for Homogeneous and Isotropic Soil

The variation of the bearing capacity coefficient with k_h for different β and φ is provided in Figs. 7 and 8, respectively. As can be noticed, regardless of the values of β and φ, N_c and N_γ decrease constantly with an increase in k_h. The decrease in N_c and N_γ with k_h tends with increasing the k_h values.

Results for Nonhomogeneous and Anisotropic Soil

The nonhomogeneous coefficient and anisotropy ratio only affect the N_c. To observe the effect of nonhomogeneous coefficient and anisotropy ratio on static bearing capacity coefficient, the anisotropy and nonhomogeneity bearing capacity factor, and the ratio of anisotropic and nonhomogeneity bearing capacity factor to isotropic and homogeneity bearing capacity factor is presented in Tables 1 and 2, respectively. This seismic bearing capacity factor for anisotropic and nonhomogeneous soils is presented in Figs. 9 and 16. Ranges of various parameters are as follows:

$$\varphi = 30\,\mathrm{and}\,40 \quad \delta = 0.5\,\mathrm{and}\,0.75 \quad \beta = 10, 20, 30, 40\,\mathrm{and}\,50$$
$$k_\mathrm{h} = 0.1, 0.2\,\mathrm{and}\,0.3 \quad \upsilon = 0, 0.5\,\mathrm{and}\,2 \quad K = 0.8\,\mathrm{and}\,2 \quad k_\mathrm{v} = 0$$

According to Table 1, N_c increases with increasing υ and decreasing K. Also, as expected, the bearing capacity increases with increasing φ and decreasing β. From Table 2, it can be concluded that when soil is homogeneous and anisotropic with the anisotropy ratio of 0.8, the N_c is 8.5% to 19% greater than that of the homogeneous and isotropic soil. Meanwhile, N_c for the homogeneous soil with an anisotropy ratio of 2 is 17.5% to 39% less than N_c of the homogeneous and isotropic soil. Hence, this difference shows that the anisotropy of soil has a considerable effect on the value of bearing capacity factor. Similar to the static condition, increasing the nonhomogeneous coefficient and decreasing the anisotropy ratio led to an increase in the seismic bearing capacity. Also, the seismic bearing capacity factor decreased with an increase in the horizontal seismic acceleration coefficient. On the other hand, when $\upsilon = 0.5$, N_c is 6% to 36% more than that of the homogeneous soil, and this difference increases to about 15% to 125% when $\upsilon = 2$. This demonstrates that the nonhomogeneity has a significant effect on N_c.

As can be seen from Figs. 9, 10, 11, 12, 13, 14, 15, and 16, when the anisotropy ratio is greater than 1 and it couples with the seismic acceleration coefficient, the value of N_c reduces drastically. Comparing all graphs in each of Figs. 9, 10, 11, 12, 13, 14, 15, and 16 demonstrates the effect of the nonhomogeneous coefficient and the anisotropy ratio on N_c. For example, it can be concluded from Fig. 9 that, when $k_\mathrm{h} = 0$ and $\beta = 10°$, N_c increases about 43% with an increase in the nonhomogeneous coefficient from 0.5 to 2, and the increase rate of N_c decreases to 17% with increasing k_h to 0.3. It means that the seismic acceleration coefficient decreases the effect of the nonhomogeneous coefficient on N_c. Furthermore, it can be found from Fig. 9 that for a constant value of the nonhomogeneous coefficient, for example $\upsilon = 0.5$ and when $k_\mathrm{h} = 0$ and $\beta = 10°$, N_c increases about 43% with decreasing the anisotropy ratio from 2 to 0.8. Under these conditions, the reduction tends to increase with an increase in the value of k_h such that it reaches 51% for $k_\mathrm{h} = 0.3$. Thus, overall, the positive effect of the nonhomogeneous coefficient and anisotropy ratio on N_c tends to decrease with an increase in k_h.

The effect of both k_h and k_v in the value of N_c is presented in Fig. 17. As we expected, the effect of both the seismic acceleration coefficients leads to a more drastic reduction in the value of N_c. The effect of k_v is exactly the same as the effect of k_h, suggesting that k_v reduces the positive effect of the nonhomogeneous coefficient and anisotropy ratio on the value of N_c.

Tables 3 and 4 indicate the effect of the nonhomogeneous coefficient and anisotropy ratio on α_A, α_B and h. Here, it is assumed that $\varphi = 10°$ and 20°, $B = 2$ m, and $k_\mathrm{h} = 0$. As can be seen from Tables 3 and 4, the active and passive angles and the depth of the failure zone decrease with increasing nonhomogeneous coefficient and anisotropy ratio. The decrease in failure depth with increasing the nonhomogeneous coefficient is in agreement with physical principles since failure takes place in the weaker upper part of the slope. To better understand the effect of anisotropy ratio and the nonhomogeneous coefficient on the location of failure surface, failure surfaces for two conditions of nonhomogeneous and anisotropy are shown

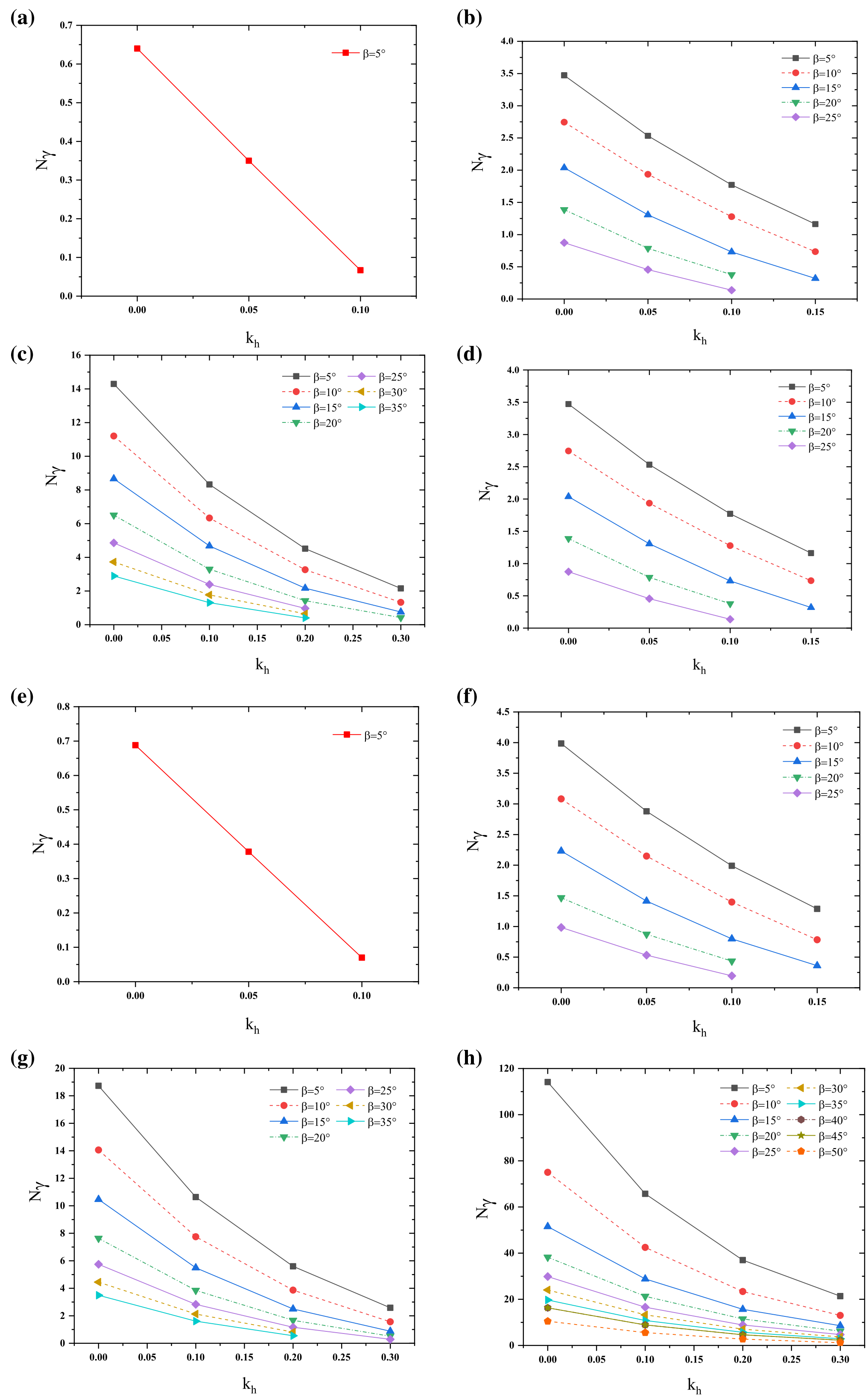

Fig. 8 Comparison of N_γ with k_h and β for **a** $\varphi = 10°$, $\delta = 0.5\varphi$; **b** $\varphi = 20°$, $\delta = 0.5\varphi$; **c** $\varphi = 30°$, $\delta = 0.5\varphi$; **d** $\varphi = 40°$, $\delta = 0.5\varphi$; **e** $\varphi = 10°$, $\delta = 0.75\varphi$ **f** $\varphi = 20°$, $\delta = 0.75\varphi$; **g** $\varphi = 30°$, $\delta = 0.75\varphi$; **h** $\varphi = 40°$, $\delta = 0.75\varphi$

in Fig. 18 using the results of Tables 3 and 4. When $\beta = 10°$ and 30° and $\varphi = 10°$ and 20°, it is clear that the active zone shrinks and the passive zone moves to the bottom of the slope with increasing the anisotropy ratio. Furthermore, when $\beta = 10°$ and $\varphi = 10°$ and 20°, both of the active and passive zones shrink with an increase in the nonhomogeneous coefficient. A similar trend is observed when $\beta = 30°$ and $\varphi = 10°$. In comparison, when $\beta = 30°$ and $\varphi = 30°$, the effect of nonhomogeneous coefficient on the pattern of active and passive zones is similar to that of the anisotropy ratio. Further computation for determining the location of the failure surface for other friction angles of soil (i.e., $\varphi = 30°$ and 40°) shows that the location of failure surface is similar to what presented in Fig. 18a–c, e.

Table 5 presents the effect of the seismic acceleration coefficient on α_A, α_B and h. Here, it is assumed that $\varphi = 20°$, $B = 2$, $K = 0.8$, $\upsilon = 0.5$, and $k_v = 0$. From Table 5, it is clear that the depth of the failure zone decreases with an increase in the seismic acceleration coefficient and increases with an increase in the slope inclination. Moreover, the active angle increases with increasing k_h, while the passive angle decreases with increasing k_h. Another result inferred from Table 5 is that the active angle increases with an increase in the slope inclination while the passive angle decreases with an increase in the slope inclination.

Figure 19 represents the location of the failure surface for different values of β and k_h. As can be seen from this figure, when the slope inclination increases, the path of failure in the passive zone deviates more than the vertical surface.

Conclusions

The effect of anisotropy and nonhomogeneity on the bearing capacity of a shallow foundation rested on an inclined ground was evaluated using a simplified Coulomb failure mechanism and the limit equilibrium method. The bearing capacity equation was presented as a function of

Table 1 Anisotropy and nonhomogeneity bearing capacity factor for static conditions

δ	υ	φ	$K = 0.8$					$K = 2$				
			β									
			10	20	30	40	50	10	20	30	40	50
0.5φ	0	10	8.874	7.89	7.041	6.281	5.616	5.526	4.798	4.233	3.812	3.534
		20	14.526	12.226	10.41	8.921	7.850	8.925	7.464	6.406	5.738	5.301
		30	26.457	20.578	16.439	13.694	11.903	15.572	12.298	10.281	9.173	8.448
		40	57.104	39.242	29.567	24.377	20.899	31.579	22.754	18.843	16.760	15.400
	0.5	10	10.792	9.423	8.291	7.336	6.653	6.141	5.246	4.579	4.150	3.870
		20	18.197	14.838	12.334	10.678	9.596	10.189	8.257	7.035	6.359	5.916
		30	33.866	24.847	19.697	16.921	15.105	18.170	13.604	11.506	10.358	9.651
		40	72.726	46.529	36.681	31.422	27.978	36.763	25.574	21.629	19.523	18.146
	2	10	15.496	13.064	11.083	10.014	9.314	7.843	6.374	5.556	5.188	4.832
		20	27.509	20.225	17.032	15.323	14.203	13.624	10.181	8.823	8.130	7.675
		30	49.124	33.683	28.496	25.617	23.726	23.253	17.126	14.973	13.819	13.062
		40	95.240	66.334	56.153	50.687	47.094	45.053	33.514	29.464	27.295	25.873
0.75φ	0	10	9.205	8.12	7.197	6.381	5.685	5.685	4.88	4.283	3.847	3.561
		20	16.018	13.174	11.006	9.313	8.184	9.557	7.841	6.645	5.924	5.452
		30	32.591	23.983	18.458	15.213	13.099	18.247	13.756	11.314	10.011	9.159
		40	89.150	54.814	39.913	32.395	27.488	45.687	30.336	25.55	22.54	20.54
	0.5	10	11.136	9.645	8.428	7.422	6.713	6.640	5.578	4.826	4.383	3.896
		20	19.820	15.758	12.861	11.069	9.898	11.612	9.016	7.646	6.914	6.072
		30	40.584	27.952	21.827	18.562	16.427	22.505	15.813	13.338	12.016	10.418
		40	103.998	64.544	48.438	42.526	37.419	50.070	35.710	29.998	28.148	23.030
	2	10	15.892	13.262	11.195	10.098	9.3750	7.998	6.442	5.602	5.153	4.859
		20	29.479	21.025	17.585	15.746	14.542	14.401	10.472	9.080	8.336	7.847
		30	55.191	37.296	31.019	27.656	25.450	25.915	18.739	16.233	14.876	13.994
		40	137.74	91.540	75.672	64.183	61.771	64.220	45.764	37.549	34.444	33.926

Table 2 Ratio of the anisotropy and nonhomogeneity bearing capacity factor to isotropic and homogeneity bearing capacity factor for static conditions

δ	υ	φ	K = 0.8					K = 2				
			β					β				
			10	20	30	40	50	10	20	30	40	50
0.5φ	0	10	1.128	1.135	1.138	1.140	1.130	0.703	0.690	0.684	0.692	0.711
		20	1.137	1.139	1.139	1.131	1.116	0.699	0.696	0.701	0.727	0.754
		30	1.152	1.149	1.141	1.122	1.105	0.678	0.687	0.714	0.752	0.784
		40	1.171	1.162	1.137	1.116	1.092	0.648	0.674	0.725	0.767	0.805
	0.5	10	1.372	1.355	1.341	1.331	1.339	0.781	0.754	0.740	0.753	0.779
		20	1.425	1.383	1.349	1.353	1.364	0.798	0.770	0.769	0.806	0.841
		30	1.475	1.387	1.367	1.386	1.402	0.791	0.760	0.799	0.849	0.896
		40	1.492	1.378	1.411	1.438	1.462	0.754	0.757	0.832	0.894	0.948
	2	10	1.970	1.879	1.792	1.817	1.875	0.997	0.917	0.898	0.941	0.973
		20	2.154	1.885	1.863	1.942	2.019	1.067	0.949	0.965	1.030	1.091
		30	2.140	1.881	1.978	2.099	2.203	1.013	0.956	1.039	1.132	1.213
		40	1.953	1.964	2.160	2.320	2.461	0.924	0.992	1.133	1.249	1.352
0.75φ	0	10	1.133	1.139	1.142	1.143	1.132	0.699	0.684	0.680	0.689	0.709
		20	1.146	1.147	1.145	1.134	1.124	0.684	0.683	0.691	0.721	0.749
		30	1.167	1.161	1.148	1.127	1.110	0.653	0.666	0.704	0.742	0.776
		40	1.190	1.169	1.112	1.084	1.104	0.610	0.647	0.712	0.754	0.825
	0.5	10	1.370	1.352	1.337	1.329	1.337	0.817	0.782	0.766	0.785	0.776
		20	1.418	1.372	1.338	1.348	1.359	0.831	0.785	0.796	0.842	0.834
		30	1.453	1.353	1.357	1.375	1.392	0.806	0.766	0.829	0.890	0.883
		40	1.388	1.376	1.349	1.423	1.503	0.668	0.761	0.836	0.942	0.925
	2	10	1.955	1.860	1.776	1.808	1.867	0.984	0.903	0.889	0.923	0.968
		20	2.109	1.831	1.830	1.917	1.997	1.030	0.912	0.945	1.015	1.078
		30	1.976	1.806	1.929	2.049	2.156	0.928	0.907	1.009	1.102	1.186
		40	1.838	1.952	2.108	2.147	2.480	0.857	0.976	1.046	1.152	1.362

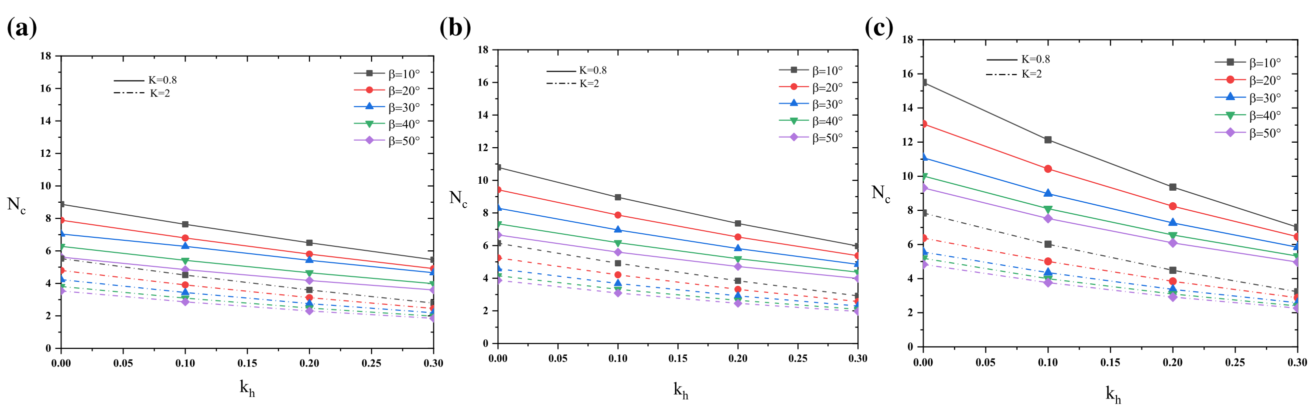

Fig. 9 Variation of N_c with k_h and β for φ = 10°, δ = 0.5φ and **a** υ = 0; **b** υ = 0.5; **c** υ = 2

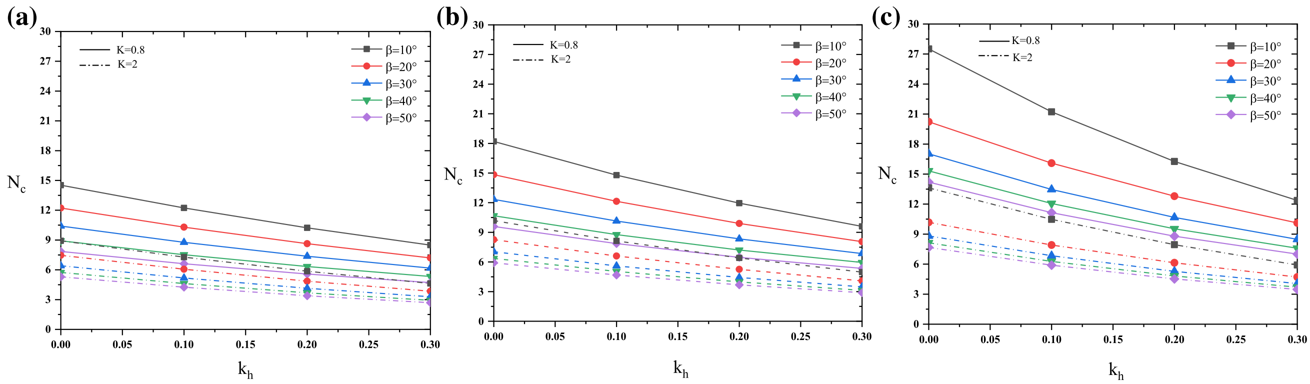

Fig. 10 Variation of N_c with k_h and β for φ = 20°, δ = 0.5φ and **a** υ = 0; **b** υ = 0.5; **c** υ = 2

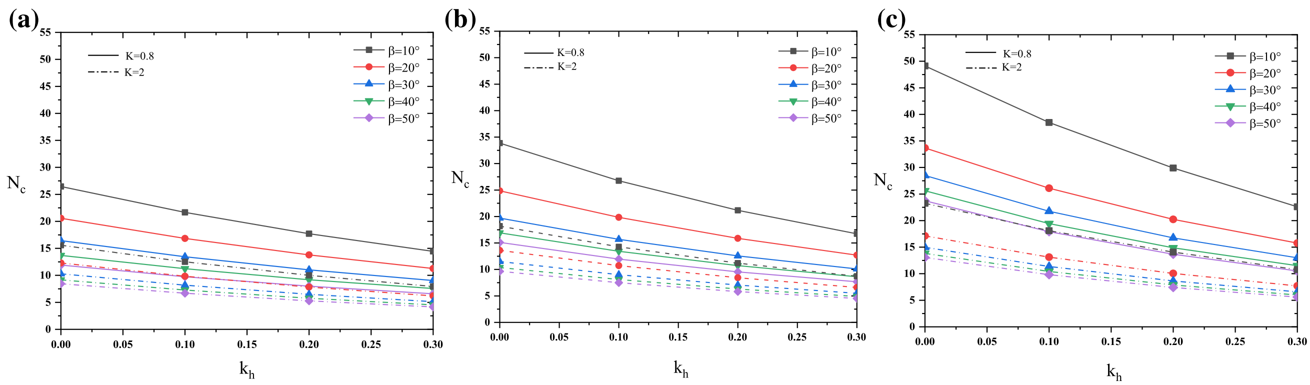

Fig. 11 Variation of N_c with k_h and β for φ = 30°, δ = 0.5φ and **a** υ = 0; **b** υ = 0.5; **c** υ = 2

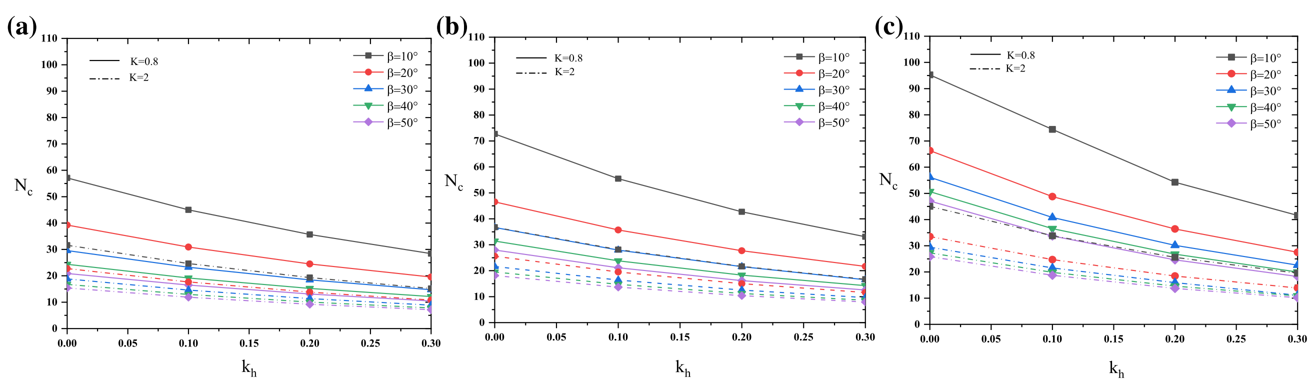

Fig. 12 Variation of N_c with k_h and β for φ = 40°, δ = 0.5φ and **a** υ = 0; **b** υ = 0.5; **c** υ = 2

slope inclination (β), friction angle (φ), anisotropy ratio (K), nonhomogeneous coefficient (υ), slip surface angle in the passive and active zone (α_A and α_B) and seismic acceleration coefficients (k_h and k_v). According to the equation provided to determine the bearing capacity of the shallow foundation, the anisotropy and nonhomogeneity only affect N_c. The main results of this study can be outlined as follows:

- A new approach for calculating the bearing capacity of nonhomogeneous and anisotropic soils on slopes can be provided using the limit equilibrium method combined with the pseudo-static seismic loading approach, and applying the simplified Coulomb failure mechanism.
- Delta (δ) is a very effective parameter in the present analysis. Given that previous researchers have presented a wide range of values for the bearing capacity factors, the present solution for δ = 0.5φ and δ = 0.75φ suggests an acceptable range for calculating bearing capacity factors.

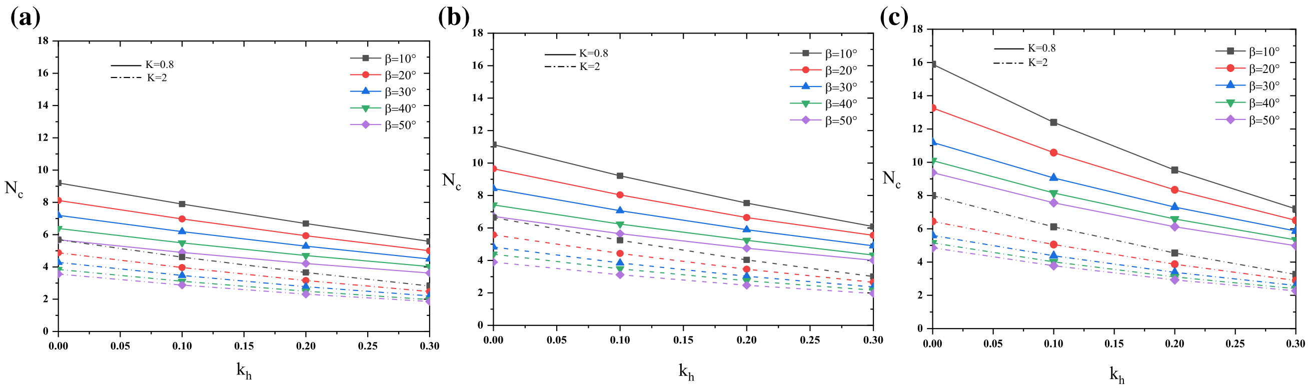

Fig. 13 Variation of N_c with k_{h} and β for φ = 10°, δ = 0.75φ and **a** υ = 0; **b** υ = 0.5; **c** υ = 2

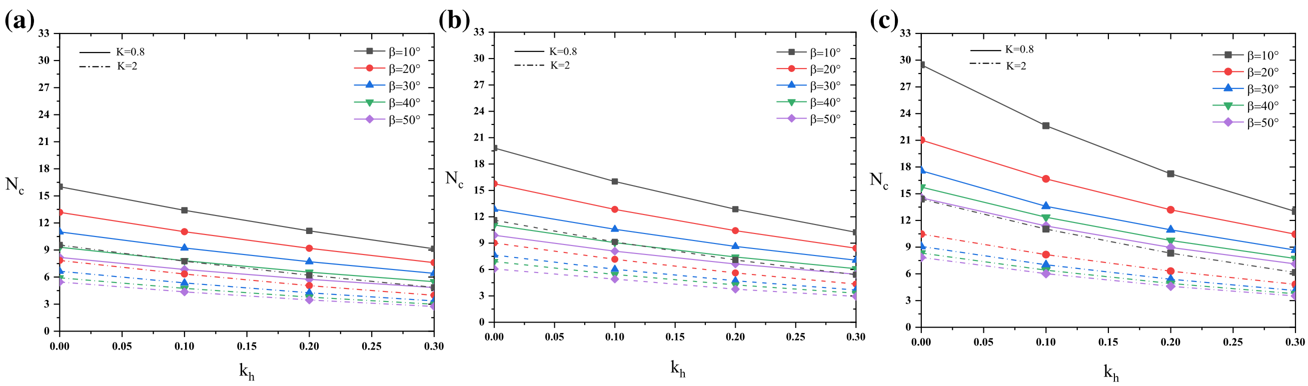

Fig. 14 Variation of N_c with k_{h} and β for φ = 20°, δ = 0.75φ and **a** υ = 0; **b** υ = 0.5; **c** υ = 2

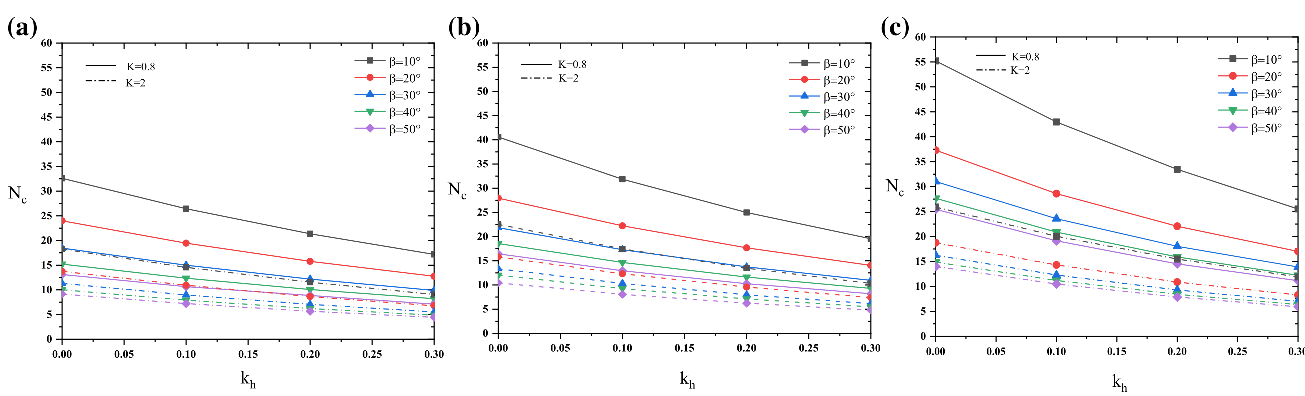

Fig. 15 Variation of N_c with k_{h} and β for φ = 30°, δ = 0.75φ and **a** υ = 0; **b** υ = 0.5; **c** υ = 2

- The bearing capacity factors N_c and N_γ decrease with increasing seismic acceleration coefficient (k_{h}) and slope inclination (β).
- N_c increases with decreasing anisotropy ratio (K) and increasing the nonhomogeneous coefficient (υ).
- The positive effect of the nonhomogeneous coefficient and anisotropy ratio on the N_c decreases with an increase in the values of k_{h} and k_{v}.
- The depth of the failure zone decreases with increasing the nonhomogeneous coefficient, the anisotropy ratio, and the seismic acceleration coefficient, while the depth

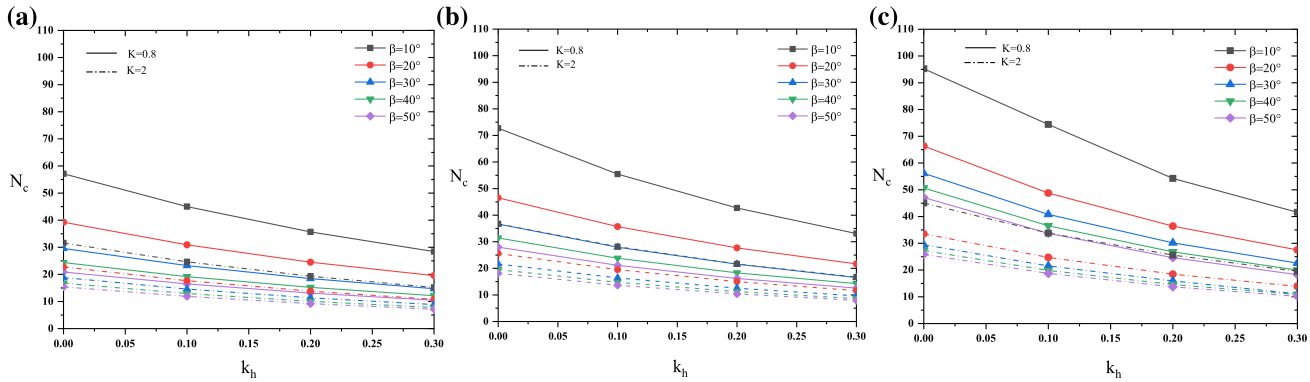

Fig. 16 Variation of N_c with k_h and β for φ = 40°, δ = 0.75φ and **a** υ = 0; **b** υ = 0.5; **c** υ = 2

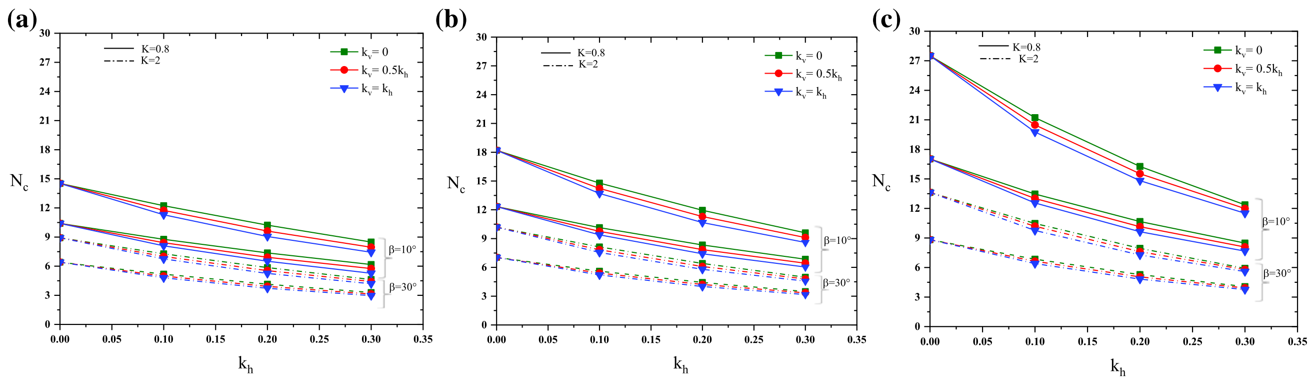

Fig. 17 Variation of N_c with k_h, k_v and β for φ = 20°, δ = 0.5φ and **a** υ = 0; **b** υ = 0.5; **c** υ = 2

Table 3 Variation of the active and passive angles and the depth of the failure zone with a constant υ for various values of K

φ	β	υ = 0.5								
		K = 0.8			K = 1			K = 2		
		α_A (°)	α_B (°)	h (m)	α_A (°)	α_B (°)	h (m)	α_A (°)	α_B (°)	h (m)
10	10	38.82	24.41	1.61	38.08	22.22	1.57	35.19	15.41	1.40
	30	40.06	6.80	1.68	39.06	4.62	1.62	35.20	− 1.09	1.42
20	10	45.93	18.07	2.07	45.66	16.61	2.05	44.47	11.77	1.96
	30	47.20	− 0.77	2.16	46.68	− 2.10	2.12	44.51	− 5.48	1.97

Table 4 Variation of the active and passive angles and the depth of the failure zone with a constant K for various values of υ

φ	β	K = 0.8								
		υ = 0			υ = 0.5			υ = 2		
		α_A (°)	α_B (°)	h (m)	α_A (°)	α_B (°)	h (m)	α_A (°)	α_B (°)	h (m)
10	10	44.52	26.05	1.97	38.82	24.41	1.61	32.76	21.75	1.29
	30	44.72	11.67	1.97	40.06	6.80	1.68	35.53	0.01	1.43
20	10	50.23	19.96	2.44	45.93	18.07	2.07	41.31	14.58	1.76
	30	50.70	5.86	2.43	47.20	− 0.77	2.16	42.82	− 7.09	1.85

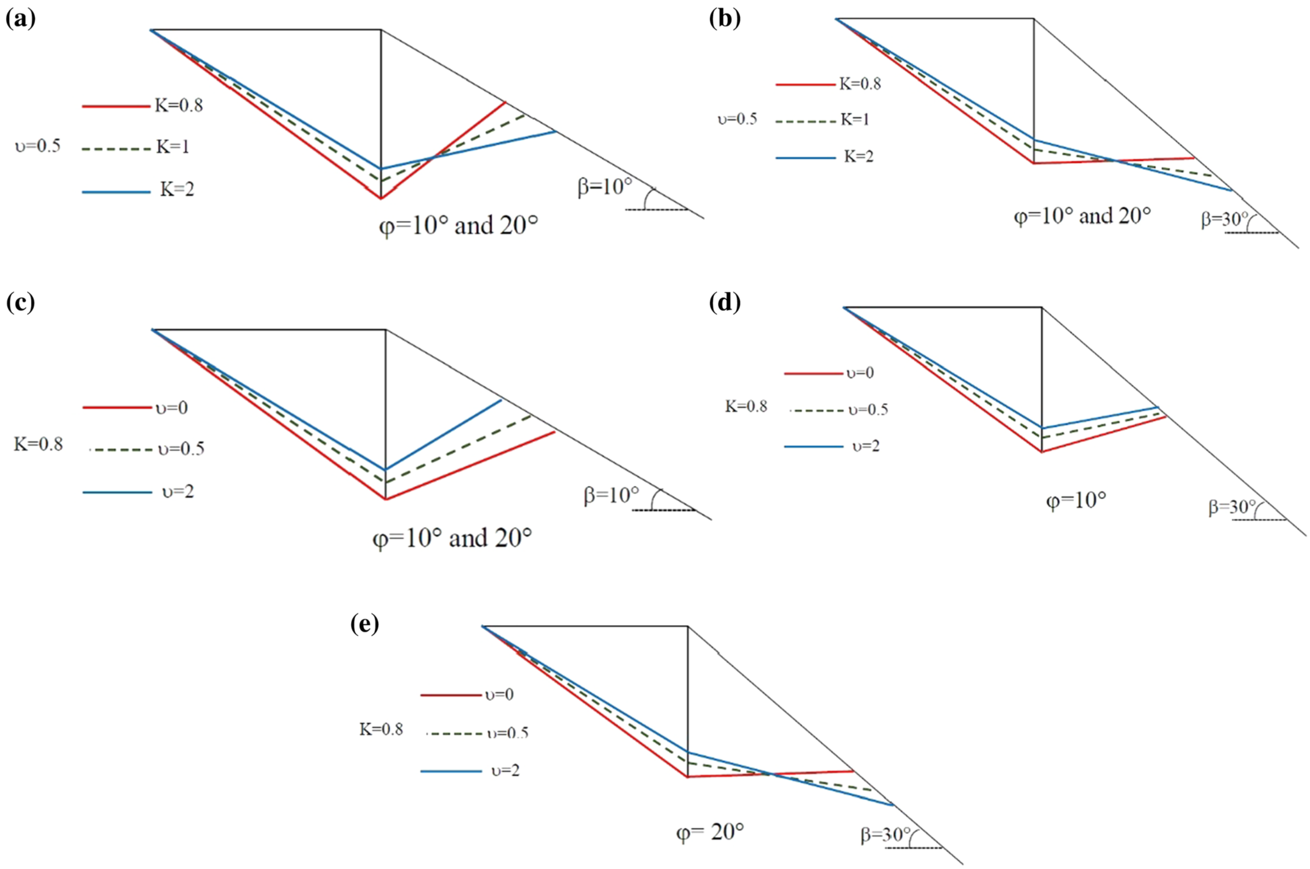

Fig. 18 Schematic demonstration of the location of failure surface for different values of anisotropy ratio for **a** φ = 10° and 20° and β = 10° and **b** φ = 10° and 20° and β = 30°; and for different values of the nonhomogeneous coefficient for **c** φ = 10° and 20° and β = 10°; **d** φ = 10° and β = 30°; **e** φ = 20° and β = 30°

Table 5 Variation of the active and passive angles and the depth of the failure zone for various values of k_h

φ	β	k_h = 0.1			k_h = 0.2			k_h = 0.3		
		α_A (°)	α_B (°)	h (m)	α_A (°)	α_B (°)	h (m)	α_A (°)	α_B (°)	h (m)
20	10	40.63	18.36	1.72	34.80	18.64	1.39	28.51	18.91	1.09
	20	41.52	9.93	1.77	36.04	10.53	1.46	30.25	11.07	1.17
	30	42.33	0.51	1.82	37.17	1.54	1.52	31.83	2.40	1.24
	40	43.04	− 10.09	1.87	38.16	− 8.48	1.57	33.26	− 7.26	1.31

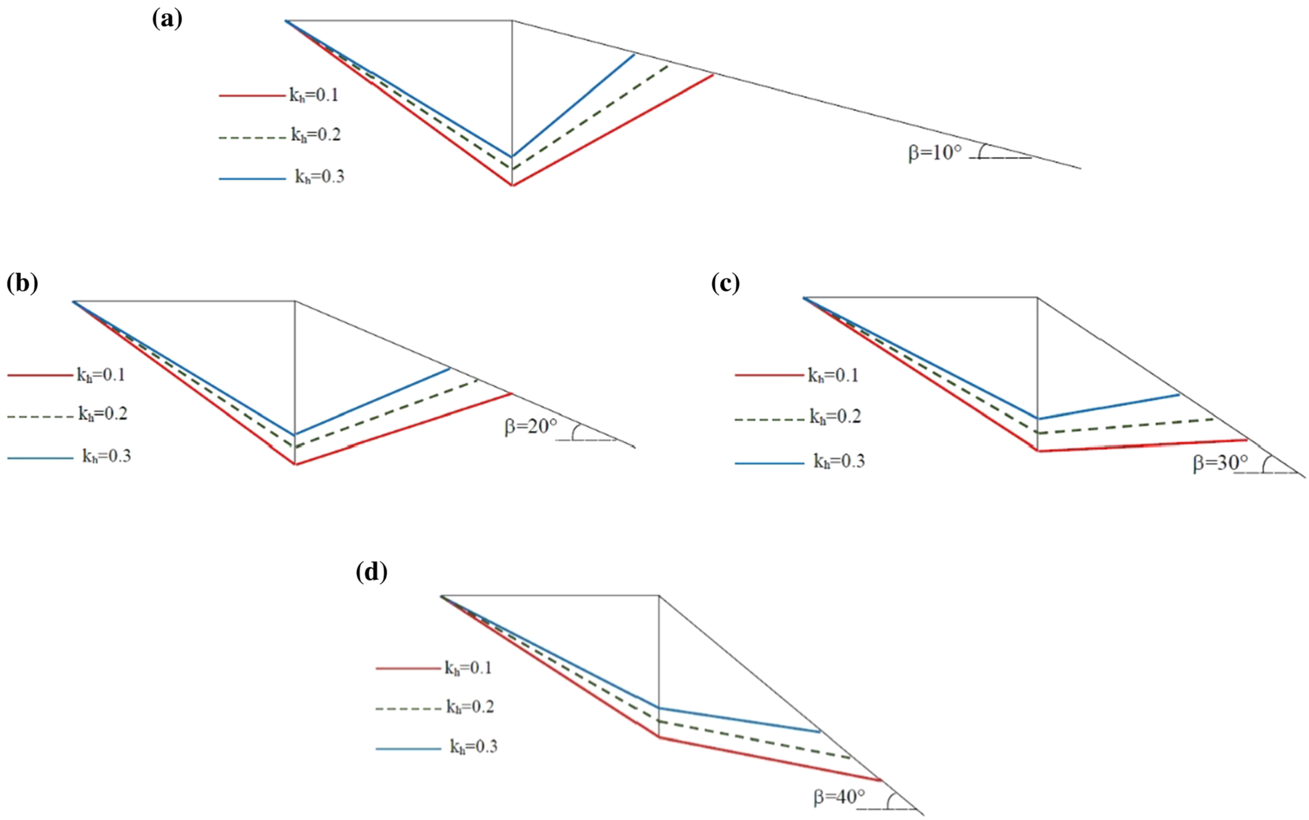

Fig. 19 Schematic demonstration of the location of failure surface for different values of the seismic acceleration coefficient for **a** β = 10°, **b** β = 20°, **c** β = 30°, and **d** β = 40°

of the failure zone increases with an increase in the slope inclination.

Funding Not applicable.

Availability of Data and Material Not applicable.

Code Availability Not applicable.

Declarations

Conflict of interest The authors declare that they have no conflict of interest.

Appendix: Analytical Functions of Eqs. (18 and 19)

$$a = \left(\frac{(1-k_v)\sin(\alpha_A-\varphi)+k_h\cos(\alpha_A-\varphi)}{\cos(\alpha_A-\varphi-\delta)}\right) \tag{23}$$

$$b = \tan\alpha_A\left[\left(\frac{\tan\alpha_A}{\tan\alpha_B+\tan\beta}\right)\left(\frac{(1-k_v)\sin(\alpha_B+\varphi)-k_h\cos(\alpha_B+\varphi)}{\cos(\alpha_B+\varphi+\delta)}\right) - \left(\frac{(1-k_v)\sin(\alpha_A-\varphi)+k_h\cos(\alpha_A-\varphi)}{\cos(\alpha_A-\varphi-\delta)}\right)\right] \tag{24}$$

$$e = \frac{1}{K}\left(1+(K-1)\sin^2\alpha_B\right)\left(\frac{\tan\alpha_A\tan\alpha_B}{\tan\alpha_B+\tan\beta}\right)\left(\frac{\sin(\alpha_B+\varphi)+\cot\alpha_B\cos(\alpha_B+\varphi)}{\cos(\alpha_B+\varphi+\delta)}\right) + (\tan\alpha_A)\frac{\sin(\alpha_B+\varphi)}{\cos(\alpha_B+\varphi+\delta)} + (\tan\alpha_A)\frac{\sin(\alpha_A-\varphi)}{\cos(\alpha_A-\varphi-\delta)} + \frac{1}{K}\left(1+(K-1)\sin^2\alpha_A\right)(\tan\alpha_A)\left(\frac{\sin(\alpha_A-\varphi)+\cot\alpha_A\cos(\alpha_A-\varphi)}{\cos(\alpha_A-\varphi-\delta)}\right) \tag{25}$$

$$f = \left(\frac{1}{K}\right)\left[(\tan\alpha_A)^2\left(\frac{\sin(\alpha_A-\varphi)+0.5\cot\alpha_A\cos(\alpha_A-\varphi)}{\cos(\alpha_A-\varphi-\delta)}\right) + \left(\frac{\tan\alpha_A\tan\alpha_B}{\tan\alpha_B+\tan\beta}\right)^2\left(\frac{0.5\sin(\alpha_B+\varphi)+0.5\cot\alpha_B\cos(\alpha_B+\varphi)}{\cos(\alpha_B+\varphi+\delta)}\right) + (\tan\alpha_A)^2\left(\frac{0.5\sin(\alpha_B+\varphi)}{\cos(\alpha_B+\varphi+\delta)}\right)\right] \tag{26}$$

References

1. Budhu M, Al-Karni A (1993) Seismic bearing capacity of soils. Geotechnique 43(1):181–187
2. Dormieux L, Pecker A (1995) Seismic bearing capacity of foundation on cohesionless soil. J Geotech Eng 121(3):300–303
3. Ghosh S, Debnath L (2017) Seismic bearing capacity of shallow strip footing with coulomb failure mechanism using limit equilibrium method. Geotech Geol Eng 35(6):2647–2661
4. Kumar J (2003) N γ for rough strip footing using the method of characteristics. Can Geotech J 40(3):669–674
5. Paolucci R, Pecker A (1997) Seismic bearing capacity of shallow strip foundations on dry soils. Soils Found 37(3):95–105

6. Richards R Jr, Elms D, Budhu M (1993) Seismic bearing capacity and settlements of foundations. J Geotech Eng 119(4):662–674
7. Sarma S, Iossifelis I (1990) Seismic bearing capacity factors of shallow strip footings. Geotechnique 40(2):265–273
8. Soubra A-H (1997) Seismic bearing capacity of shallow strip footings in seismic conditions. Proc Inst Civ Eng Geotech Eng 125(4):230–241
9. Soubra A-H (1999) Upper-bound solutions for bearing capacity of foundations. J Geotech Geoenviron Eng 125(1):59–68
10. Zhu D (2000) The least upper-bound solutions for bearing capacity factor Nγ. Soils Found 40(1):123–129
11. Halder K, Chakraborty D, Kumar Dash S (2019) Bearing capacity of a strip footing situated on soil slope using a non-associated flow rule in lower bound limit analysis. Int J Geotech Eng 13(2):103–111
12. Hansen JB (1970) A revised and extended formula for bearing capacity
13. Meyerhof G (1957) The ultimate bearing capacity of foundations on slopes. In: Proc., 4th int. conf. on soil mechanics and foundation engineering, pp 384–386
14. Azzouz AS, Baligh MM (1983) Loaded areas on cohesive slopes. J Geotech Eng 109(5):724–729
15. Castelli F, Motta E (2010) Bearing capacity of strip footings near slopes. Geotech Geol Eng 28(2):187–198
16. Chen C-f, Dong W-z, Tang Y-z (2007) Seismic ultimate bearing capacity of strip footings on slope. J Cent South Univ Technol 14(5):730
17. Choudhury D, Subba Rao K (2006) Seismic bearing capacity of shallow strip footings embedded in slope. Int J Geomech 6(3):176–184
18. Kovalev I (1964) De la resistance ultime des fondations limitees par un talus. Traduction du russe Extrait du recueil des travaux de LIIZLT, fascicule 225
19. Kumar J, Kumar N (2003) Seismic bearing capacity of rough footings on slopes using limit equilibrium. Geotechnique 53(3):363–369
20. Mizuno T, TOKUMITSU Y, Kawakami H, (1960) On the bearing capacity of a slope of cohesionless soil. Soils Found 1(2):30–37
21. Narita K, Yamaguchi H (1990) Bearing capacity analysis of foudations on slopes by use of log-spiral sliding surfaces. Soils Found 30(3):144–152
22. Sarma S, Chen Y (1996) Bearing capacity of strip footings near sloping ground during earthquakes. In: Proceedings of the 11th world conference on earthquake engineering, Acapulco
23. Kumar J, Mohan Rao V (2003) Seismic bearing capacity of foundations on slopes. Geotechnique 53(3):347–361
24. Graham J, Andrews M, Shields D (1988) Stress characteristics for shallow footings in cohesionless slopes. Can Geotech J 25(2):238–249
25. Giroud J (1971) Force portante d'une fondation sur une pente. ANN ITBTP-SERIE: THEORIES ET METHODES DE CALCUL NO 142 (283/284)
26. Andrews M (1986) Computation of bearing capacity coefficients for shallow footings on cohesionless slopes using stress characteristics
27. Kumar J, Chakraborty D (2013) Seismic bearing capacity of foundations on cohesionless slopes. J Geotech Geoenviron Eng 139(11):1986–1993
28. Chakraborty D, Kumar J (2015) Seismic bearing capacity of shallow embedded foundations on a sloping ground surface. Int J Geomech 15(1):04014035
29. Chakraborty D, Kumar J (2013) Bearing capacity of foundations on slopes. Geomech Geoeng 8(4):274–285
30. Mofidi Rouchi J, Farzaneh O, Askari F (2014) Bearing capacity of strip footings near slopes using lower bound limit analysis. Civ Eng Infrastruct J 47(1):89–109
31. Shiau J, Merifield R, Lyamin A, Sloan S (2011) Undrained stability of footings on slopes. Int J Geomech 11(5):381–390
32. Chakraborty D, Mahesh Y (2016) Seismic bearing capacity factors for strip footings on an embankment by using lower-bound limit analysis. Int J Geomech 16(3):06015008
33. Askari F, Farzaneh O (2003) Upper-bound solution for seismic bearing capacity of shallow foundations near slopes. Geotechnique 53(8):697–702
34. Georgiadis K (2010) Undrained bearing capacity of strip footings on slopes. J Geotech Geoenviron Eng 136(5):677–685
35. Kumar J, Ghosh P (2006) Seismic bearing capacity for embedded footings on sloping ground. Geotechnique 56(2):133–140
36. KuSakabe O, Kimura T, Yamaguchi H (1981) Bearing capacity of slopes under strip loads on the top surfaces. Soils Found 21(4):29–40
37. Leshchinsky B, Xie Y (2017) Bearing capacity for spread footings placed near c'-ϕ' slopes. J Geotech Geoenviron Eng 143(1):06016020
38. Sawada T, NomachiChen SGW-F (1994) Seismic bearing capacity of a mounded foundation near a down-hill slope by pseudo-static analysis. Soils Found 34(1):11–17
39. Yamamoto K (2010) Seismic bearing capacity of shallow foundations near slopes using the upper-bound method. Int J Geotech Eng 4(2):255–267
40. Bishop AW (1966) The strength of soils as engineering materials. Geotechnique 16(2):91–130
41. Casagrande A (1944) Shear failure of anisotropic materials. Proc Boston Soc Civ Eng 31:74–87
42. Livneh M, Komornik A (1967) Anisotropic strength of compacted clays. In: Asian conf soil mech and fdn e proc/is
43. Skempton A (1948) Vane tests in the alluvial plain of the River Forth near Grangemouth. Geotechnique 1(2):111–124
44. Pakdel P, Jamshidi Chenari R, Veiskarami M (2019) Seismic bearing capacity of shallow foundations rested on anisotropic deposits. Int J Geotech Eng 15:1–12
45. Al-Shamrani MA, Moghal AAB (2012) Upper bound solutions for bearing capacity of footings on anisotropic cohesive soils. In: GeoCongress 2012: state of the art and practice in geotechnical engineering, pp 1066–1075
46. Al-Shamrani MA (2005) Upper-bound solutions for bearing capacity of strip footings over anisotropic nonhomogeneous clays. J Jpn Geotech Soc Soils Found 45(1):109–124
47. Davis E, Booker J (1973) The effect of increasing strength with depth on the bearing capacity of clays. Geotechnique 23(4):551–563
48. Davis EH, Christian JT (1970) Bearing capacity of anisotropic cohesive soil
49. Gourvenec S, Randolph M (2003) Effect of strength non-homogeneity on the shape of failure envelopes for combined loading of strip and circular foundations on clay. Géotechnique 53(6):575–586
50. Izadi A, Nazemi Sabet Soumehsaraei M, Jamshidi Chenari R, Ghorbani A (2019) Pseudo-static bearing capacity of shallow foundations on heterogeneous marine deposits using limit equilibrium method. Mar Georesour Geotechnol 37(10):1163–1174
51. Menzies B (1976) An approximate correction for the influence of strength anisotropy on conventional shear vane measurements used to predict field bearing capacity. Geotechnique 26(4):631–634
52. Raymond GP (1967) The bearing capacity of large footings and embankments on clays. Geotechnique 17(1):1–10
53. Reddy AS, Rao KV (1981) Bearing capacity of strip footing on anisotropic and nonhomogeneous clays. Soils Found 21(1):1–6
54. Reddy AS, Sriniuasan R (1970) Bearing capacity of footings on anisotropic soils. J Soil Mech Found Div 96(6):1967–1986

55. Reddy AS, Srinivasan R (1967) Bearing capacity of footings on layered clays. J Soil Mech Found Div 93(2):83–99
56. Reddy AS, Srinivasan R (1971) Bearing capacity of footings on clays. Soils Found 11(3):51–64
57. Salencon J (1974) Bearing capacity of a footing on a φ= 0 soil with linearly varying shear strength. Geotechnique 24(3):443–446
58. Yang X-L, Du D-C (2016) Upper bound analysis for bearing capacity of nonhomogeneous and anisotropic clay foundation. KSCE J Civ Eng 20(7):2702–2710
59. Chen W-F (2013) Limit analysis and soil plasticity. Elsevier
60. Skempton A (1951) The bearing capacity of clays. In: Selected papers on soil mechanics, pp 50–59
61. Sreenivasulu V, Ranganatham B (1971) Bearing Capacity of anisotripy nonhomogenous medium under φ= 0 condition. Soils Found 11(2):17–27
62. Meyerhof G (1978) Bearing capacity of anisotropic cohesionless soils. Can Geotech J 15(4):592–595
63. Reddy AS, Rao KV (1982) Bearing capacity of strip footing on c-ψ soils exhibiting anisotripy and nonhomogeneity in cohesion. Soils Found 22(1):49–60
64. Halder K, Chakraborty D (2019) Seismic bearing capacity of a strip footing over an embankment of anisotropic clay. Front Built Environ 5:134
65. Ghazavi M, Eghbali AH (2008) A simple limit equilibrium approach for calculation of ultimate bearing capacity of shallow foundations on two-layered granular soils. Geotech Geol Eng 26(5):535–542
66. Livneh M, Greenstein J (1972) The bearing capacity of footings on nonhomogeneous clays. Bruner Institute of Transportation, Technion Research and Development Foundation Limited
67. Tant K, Craig W (1995) Bearing capacity of circular foundations on soft clay of strength increasing with depth. Soils Found 35(4):21–35
68. Wood DM (2003) Geotechnical modelling, vol 1. CRC Press
69. Kennedy J, Eberhart R (1995) Particle swarm optimization. In: Proceedings of ICNN'95-international conference on neural networks. IEEE, pp 1942–1948
70. Debnath L, Ghosh S (2018) Pseudostatic analysis of shallow strip footing resting on two-layered soil. Int J Geomech 18(3):04017161
71. Debnath L, Ghosh S (2019) Pseudo-static bearing capacity analysis of shallow strip footing over two-layered soil considering punching shear failure. Geotech Geol Eng 37(5):3749–3770
72. Vesic AS (1973) Analysis of ultimate loads of shallow foundations. J Soil Mech Found Div 99(1):45–73